ChemComm

RSC Publishing

COMMUNICATION

View Article Online
View Journal | View Issue

Designer nanojunctions: orienting shaped nanoparticles within polymer thin-film nanocomposites†

Cite this: *Chem. Commun.*, 2013, **49**, 4382

Received 1st October 2012,
Accepted 23rd November 2012

DOI: 10.1039/c2cc37158h

www.rsc.org/chemcomm

Bo Gao, Yahya Alvi, David Rosen, Marvin Lav and Andrea R. Tao*

We demonstrate that polymer-grafted metal nanoparticles of various shapes and dimensions self-assemble into arrays of string-like superstructures upon phase separation within a matrix polymer. Interparticle orientation within these nanocomposites can be dictated by the chain length of the grafted polymer.

Noble metal nanoparticles (NP) that support localized surface plasmon resonances have attracted attention due to their ability to control and manipulate light at nanoscale dimensions. Research efforts have been made toward organizing shaped NPs into hierarchically ordered structures such as extended NP superlattices, arrays, and networks.[1–3] In many cases, highly one-dimensional (1D) superstructures of metal NPs with nanometer-sized interstitial gaps are desired. Within the nanojunction gap formed by neighboring NPs, the electromagnetic field is highly intensified due to light confinement. The degree and manner of light confinement depend dramatically on the interparticle orientation and gap distance for the nanojunction, and are of great importance for applications such as surface-enhanced Raman spectroscopy and metamaterials.

Self-assembly can enable the large-scale fabrication of nanojunction arrays through the organization of metal NPs within polymer films. We previously demonstrated that polymer-grafted metal NPs embedded within a polymer matrix can undergo self-assembly and self-orientation without any face-selective chemical modification of the NP surface.[4] Silver nanocubes grafted with hydrophilic polymers were organized into arrays of 1D strings within a hydrophobic polystyrene matrix film. Depending on the length of the grafted polymer chain, nanocubes could be assembled through either edge–edge or face–face interactions by tailoring the attractive van der Waals (vdW) and repulsive steric forces between neighboring NPs.

Here, we apply this facile self-assembly approach to a variety of metal NP shapes, including spherical NPs, nanorods, and triangular nanoprisms. These NPs possess highly regular shapes that have the potential to result in nanojunctions with specific coordination geometries (*e.g.* linear or trigonal assemblies) based on their number of vertexes as depicted in Fig. 1. Nanospheres possess no vertexes, nanorods possess two vertexes, and nanoprisms possess three vertexes, all with the potential to self-assemble into string or island like superstructures upon nanocomposite phase separation. These NPs also possess unique surface plasmon resonance signatures that correspond to their shape, making them ideal candidates for constructing nanojunctions with tailored plasmonic properties.

During the assembly process, NP orientation is dictated by two factors, as established by our earlier work on silver nanocubes: the directional interparticle interactions provided by the NP shape and the chain length of the grafted polymer.[4] ''Bare'' metal nanoparticles are expected to experience a net attractive potential for assembly due to vdW forces. Polymer grafts introduce steric repulsion between two closely-spaced nanoparticles, generated by chain compression as the nanoparticles approach with each other. These repulsion forces can be modulated by chain length. When grafted with short polymer chains, the NPs adopt side–side orientations favored by strong vdW interactions. When grafted with long polymer chains, the NPs favor vertex–vertex orientation which alleviates the steric repulsion between adjacent, closely-spaced NPs.

First, we demonstrate the assembly of spherical NPs within a homopolymer matrix (Fig. 2a) We synthesized well-dispersed spherical gold NPs (diameter = 13 nm) according to Turkevich method.[5] The NPs were coated with a long polymer graft of poly(vinyl pyrrolidone) (PVP) with a M_w = 55 k and a final graft layer thickness of 15 ± 1 nm as measured by dynamic light scattering. The NPs were then distributed at an air–water interface to facilitate transfer onto a supported polystyrene (PS, M_w = 11 k) thin-film. Upon exposure to chloroform vapor, the well-separated nanoparticles (Fig. 2c) sink into the hydrophobic polymer matrix. This is followed by spontaneous phase segregation into 1D superstructures that are a single-NP wide (Fig. 2d).

NanoEngineering Department, University of California, San Diego, 9500 Gilman Dr #0448, La Jolla, CA 92093-0448, USA. E-mail: atao@ucsd.edu; Fax: +1-858-5349553; Tel: +1-858-8224237

† This article is part of the *ChemComm* 'Emerging Investigators 2013' themed issue.

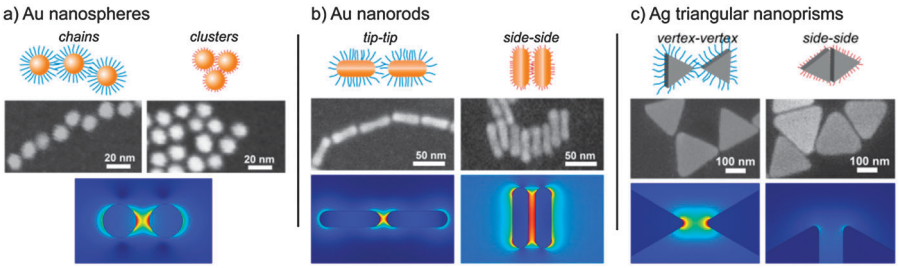

Fig. 1 Schematics, SEM images, and electrodynamic simulations of (a) Au nanosphere, (b) Au nanorod, (c) Ag triangular nanoprism assemblies. The color scale for the simulation results correspond to electromagnetic near-field amplitude (E) with respect to the incident field, E_o when excited at the resonant surface plasmon frequencies. Dark blue corresponds to $E = 0$ V m^{-1} and red corresponds to an E of (a) 17 E_o for spheres, (b)130 E_o for tip–tip nanorods and 4.5 E_o for side–side nanorods, and (c) 2000 E_o for both vertex–vertex and side–side nanoprisms.

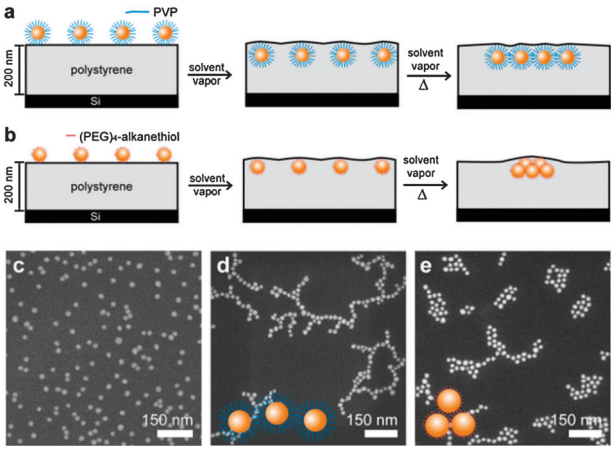

Fig. 2 Schematic of Au nanosphere self-assembly in PS film upon solvent annealing. (a) Long-chain PVP-coated Au NPs embed and self-assemble into string like structures; (b) Short-chain $(PEG)_4$ alkanethiol coated Au NPs embed and self-assemble into cluster like structures. SEM images of (c) Au NPs deposited on PS film before anneal; resulting films of Au NPs coated with (d) long PVP chains and (e) short $(PEG)_4$-alkanethiols.

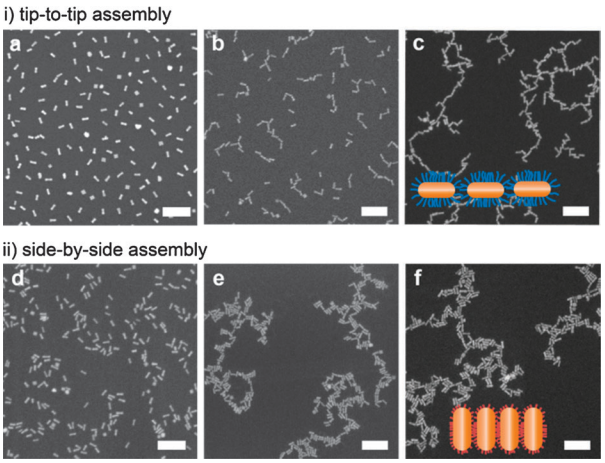

Fig. 3 SEM images of assembled Au nanorods. Long-chain PVP-coated nanorods after solvent annealing for (a) 0 min and (b) 110 min. (c) SEM image of the network formed at high nanorod loading density. Short $(PEG)_4$-alkanethiol coated nanorods (d) before annealing, (e) after solvent annealing for 145 min and (f) heated for 4 hours at 110 °C after solvent annealing to form side-to side NP aggregates. Scale bar is 200 nm.

Because the spherical NPs are totally isotropic in shape and surface chemistry, the formation of these string structures is somewhat surprising. Previous reports for polystyrene grafted silica nanospheres (diameter = 14 nm) have suggested that these superstructures are achieved through dipole-like interactions caused by rearrangement of the polymer grafts at the NP surface.[1,6] These studies demonstrated that polymer graft length is a key parameter in dictating superstructure morphology, which can be modulated from aggregates to sheets to strings.[1,7] To demonstrate the importance of the polymer graft length in our nanocomposite system, we grafted the spherical gold NPs with a short polymer graft composed of (11-mercapto-undecyl) tetra(ethylene glycol). This alkanethiol is terminated with a short four-unit PEG chain with a total chain length of approximately 2.0 nm.[8] Upon solvent annealing, these NPs form island-like clusters during the phase segregation process (Fig. 3e). This higher NP packing density is consistent with a decrease in steric repulsion between the polymer grafts attached to neighboring NPs.

Next, we demonstrate the oriented assembly of gold nanorods, which are known to display dipolar surface plasmon resonances corresponding the long and short axes of the nanorod.[9] Nanorods have been widely explored as building blocks for extended chains and network structures in both polymer blends and within colloidal dispersions.[10–12] Here, we show that nanorods can be assembled with tip–tip orientations in a homopolymer matrix and without site-selective chemical functionalization (Fig. 3). Gold nanorods (12 nm wide and 45 nm long) were synthesized by seed-mediated growth[13] and coated with long PVP polymer chains (M_w = 55 K). The phase segregation process results in the assembly of nanorods into extended 1D superstructures (Fig. 3b and c) where 82.1 ± 1.0% of the assembled nanorods adopt tip–tip (TT) orientations and 9 ± 1.6% adopt side–side (SS) orientations.

The slow diffusion rate of nanorods in the high viscosity polymer matrix allows us to carry out time-dependent observations of the assembly process. We analyzed nanorod–polymer composite films at different stages of assembly by removing films from the solvent vapor, which effectively solidifies the polymer matrix and traps the dynamic 1D superstructures. At early stages of 1D string formation, well-separated nanorods aggregate to form short chains consisting of only a few nanorods (Fig. 3b). As assembly proceeds, these short chains grow by

merging with neighboring chains (Fig. 3c). This is different from other mechanisms where strings nucleate and slowly grow through the end-attachment of single nanorods.[14]

To demonstrate the influence of the graft polymer on nanorod orientation, we modified the gold nanorods with short PEGylated alkanethiol grafts. As shown in Fig. 3e when these PEGylated nanorods are assembled within the homopolymer composite, they adopt the SS configuration with a 46.3 ± 2.9% occurrence and the TT configuration with a 33.4 ± 2.1% occurrence. The nanorod chains are composed of linked nanorods bundles that are 2–3 NPs thick, which we attribute to the reduced steric repulsion stemming from the shorter grafts. In contrast with our previous observations for nanocubes, the relatively low ratio of SS-oriented nanorods is likely due to kinetically trapped orientations. We suspect that rotation is severely limited by the high aspect-ratio of the nanorods (~3.8) and that the nanorods possess a high energy barrier for reorientation. This is evidenced by nanocomposite films that were subjected to thermal annealing above T_g of the polystyrene matrix and do not exhibit signs of nanorod reorientation or reordering (Fig. 3f).

We also demonstrate the oriented assembly of silver triangular nanoprisms, which we expect to form hierarchical superstructures dominated by vertex–vertex NP orientations. The nanoprisms (side length = 250 nm and thickness = 10 nm) were synthesized by colloidal methods.[15] We carried out surface modification of the nanoprisms with a long thiol-terminated polyethylene glycol (PEG) graft (M_w = 54 k) and deposited the prisms onto a supported polystyrene film (Fig. 4a). Upon solvent annealing, nanoprisms assemble into string-like structures. Coordination through nanoprism vertexes (Fig. 4b) are favored, with 52.1 ± 2.0% of the nanojunctions resembling bow-tie junctions. Reorientation of the prisms into side-by-side orientations can be promoted with a shorter polymer graft, where these orientations are observed with a 49.8 ± 1.7% occurrence.

Many of the triangular nanoprisms appear to be trapped in orientations where the nanoprisms are rotated off of the junction axis. We account for these defects by considering the nanoprism geometry. First, the nanoprism shape does not allow for high polymer compression. Because the nanoprisms are quite thin, polymer chains are able to escape physical confinement within the nanoparticle junction, leading to alleviated steric repulsion during the assembly process. Thus, tailoring graft length may not modulate nanoprism interactions as effectively as with other shapes. Second, many of these defect orientations are caused by imperfections in shape. For example, nanoprisms synthesized by colloidal methods are known to possess highly rounded corners. Polymers grafted to vertexes with a larger radius of curvature experience less steric repulsion upon assembly, which can lead to misorientation. However, these defects have the potential to be ameliorated by introducing additional attractive or repulsive interactions between grafted chains and the nanoprism surface.

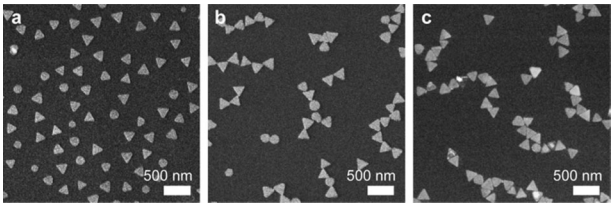

Fig. 4 SEM images of Ag triangular nanoprisms in the nanocomposite film (a) before annealing, and after annealing for prisms grafted with (b) PEG-thiol (M_w = 54 k) and (c) short $(PEG)_4$-alkanethiols.

In summary, we demonstrate the ability to fabricate large-area nanocomposites where metal NPs of varying size, shape, and valence spontaneously organize into oriented nanojunctions. The nature of this NP assembly is highly dependent on NP–polymer interfacial interactions and interparticle interactions, and the presence of assembly defects or misorientation can be attributed directly to NP building block dimensions. This approach is highly versatile with the potential to be extended towards non-metallic NPs such as semiconductor quantum dots or dielectric NPs, facilitating fabrication of engineered nanocomposites that exhibit well-defined structure–property relationships.

This work was supported through a grant from the Office of Naval Research (Award No. N000141210574), and a grant from the National Science Foundation (CMMI, Award No. 1200850).

Notes and references

1 P. Akcora, H. Liu, S. K. Kumar, J. Moll, Y. Li, B. C. Benicewicz, L. S. Schadler, D. Acehan, A. Z. Panagiotopoulos, V. Pryamitsyn, V. Ganesan, J. Ilavsky, P. Thiyagarajan, R. H. Colby and J. F. Douglas, *Nat. Mater.*, 2009, **8**, 354–359.
2 S. C. Glotzer and M. J. Solomon, *Nat. Mater.*, 2007, **6**, 557–562.
3 Z. Nie, A. Petukhova and E. Kumacheva, *Nat. Nanotechnol.*, 2009, **5**, 15–25.
4 B. Gao, G. Arya and A. R. Tao, *Nat. Nanotechnol.*, 2012, **7**, 433–437.
5 J. Turkevich, P. C. Stevenson and J. Hillier, *Discuss. Faraday Soc.*, 1951, **11**, 55–75.
6 J. B. Hooper, D. Bedrov and G. D. Smith, *Langmuir*, 2008, **24**, 4550–4557.
7 D. Maillard, S. K. Kumar, A. Rungta, B. C. Benicewicz and R. E. Prud'homme, *Nano Lett.*, 2011, **11**, 4569–4573.
8 B. Zhu, T. Eurell, R. Gunawan and D. Leckband, *J. Biomed. Mater. Res.*, 2001, **56**, 406–416.
9 K. G. Thomas, S. Barazzouk, B. I. Ipe, S. T. S. Joseph and P. V. Kamat, *J. Phys. Chem. B*, 2004, **108**, 13066–13068.
10 J. A. H. Michael and L. Mohamed, *J. Chem. Phys.*, 2008, **108**, 054901.
11 Z. Nie, D. Fava, E. Kumacheva, S. Zou, G. C. Walker and M. Rubinstein, *Nat. Mater.*, 2007, **6**, 609–614.
12 K. Liu, N. Zhao and E. Kumacheva, *Chem. Soc. Rev.*, 2011, **409**, 656–671.
13 N. R. Jana, L. Gearheart and C. J. Murphy, *Adv. Mater.*, 2001, **13**, 1389–1393.
14 K. Liu, Z. Nie, N. Zhao, W. Li, M. Rubinstein and E. Kumacheva, *Science*, 2010, **329**, 197–200.
15 G. S. Métraux and C. A. Mirkin, *Adv. Mater.*, 2005, **17**, 412–415.

